# The Bénard Problem of Rarefied Gas Dynamics

Yoshio Sone, Kazuo Aoki, Hiroshi Sugimoto, and Hideto Motohashi

（曾根良夫，青木一生，杉元　宏，本橋秀人）

Division of Aeronautics and Astronautics,

Graduate School of Engineering, Kyoto University,

Kyoto 606-01, Japan

## Abstract

The two-dimensional Bénard problem of a rarefied gas in a rectangular domain is studied numerically by a finite-difference analysis of the Boltzmann-Krook-Welander equation. The diffuse reflection is assumed on the upper cooled wall and on the lower heated wall and the specular reflection on the side boundaries. The range of the parameters where a convection exists, steady flow patterns, a bifurcation of flow pattern, and a process of convergence to an array of uniform size rolls are presented.

## I. Introduction

The Bénard problem concerning the instability of a layer of fluid heated from below has long been of interest to many scientists and engineers, and a lot of works have been done on the basis of the continuum theory[1-5]. The study of the problem of a rarefied gas is just at a starting point, and only a few works[6], which their authors call preliminary, have been done by the direct simulation Monte Carlo method[7,8]. In a series of papers we will study the problem more systematically and try to obtain more comprehensive result of the problem. In the present paper we consider the two-dimensional Bénard problem of a rarefied gas in a rectangular domain and investigate the condition (the range of the parameters included in the problem) that allows a state with flow, flow patterns, and bifurcation of

flow. Numerical analysis by a finite-difference method on the basis of the Boltzmann-Krook-Welander equation[8-10] is chosen to pursue the problem.

## II.  Problem and basic equation

In this paper we consider two dimensional flows of a rarefied gas in a rectangular domain $(0 < X_1 < L, 0 < X_2 < D$; $X_i$ is the Cartesian coordinate system), where the gas is subject to a uniform gravitational force in the negative $X_2$ direction, the lower boundary at $X_2 = 0$ is heated at a uniform temperature $T_h$, and the upper at $X_2 = D$ is cooled at a uniform temperature $T_c$. We analyze the behavior of the gas under the following assumptions:

i) The behavior of the gas is described by the Boltzmann-Krook-Welander equation.

ii) The molecules make the diffuse reflection on the upper and lower boundaries.

iii) The molecules make the specular reflection on the side boundaries at $X_1 = 0$ and $L$.

The Boltzmann-Krook-Welander equation is given by

$$\frac{\partial f}{\partial t} + \xi_1 \frac{\partial f}{\partial X_1} + \xi_2 \frac{\partial f}{\partial X_2} - g \frac{\partial f}{\partial \xi_2} = A_c \rho (f_e - f), \tag{1}$$

$$f_e = \frac{\rho}{(2\pi RT)^{3/2}} \exp(-\frac{(\xi_i - v_i)^2}{2RT}), \tag{2}$$

$$\rho = \int f d\xi_1 \, d\xi_2 \, d\xi_3, \tag{3a}$$

$$v_i = \rho^{-1} \int \xi_i f d\xi_1 \, d\xi_2 \, d\xi_3, \tag{3b}$$

$$3RT = \rho^{-1} \int (\xi_i - v_i)^2 f d\xi_1 \, d\xi_2 \, d\xi_3. \tag{3c}$$

Here, the notations are as follows: $t$ is the time; $\xi_i$ is the molecular velocity; $f$ is the velocity distribution function; $\rho$ is the density of the gas; $v_i$ is the flow velocity ($v_3 = 0$) of the gas; $T$ is the temperature of the gas; $g$ is the acceleration of gravity; $A_c$ is a constant ($A_c \rho$ is the collision frequency of a molecule, which is common to all the molecules in the case of the Boltzmann-Krook-Welander model); $R$ is the specific gas constant. The integrals in Eqs. (3a)–(3c) are carried out over the whole $\xi_i$ space.

The boundary conditions on the upper and lower boundaries are, at $X_2 = 0$,

$$f = \rho_h (2\pi RT_h)^{-3/2} \exp(-\xi_i^2 / 2RT_h), \qquad (\xi_2 > 0), \tag{4a}$$

$$\rho_h = -(2\pi / RT_h)^{1/2} \int_{\xi_2 < 0} \xi_2 f d\xi_1 \, d\xi_2 \, d\xi_3, \tag{4b}$$

and, at $X_2 = D$,

$$f = \rho_c (2\pi RT_c)^{-3/2} \exp(-\xi_i^2 / 2RT_c), \qquad (\xi_2 < 0), \tag{5a}$$

$$\rho_c = (2\pi / RT_c)^{1/2} \int_{\xi_2 > 0} \xi_2 f d\xi_1 \, d\xi_2 \, d\xi_3. \tag{5b}$$

The boundary conditions on the side boundaries are, at $X_1 = 0$,

$$f(X_1, X_2, t, \xi_1, \xi_2, \xi_3) = f(X_1, X_2, t, -\xi_1, \xi_2, \xi_3), \qquad (\xi_1 > 0), \tag{6}$$

and, at $X_1 = L$,

$$f(X_1, X_2, t, \xi_1, \xi_2, \xi_3) = f(X_1, X_2, t, -\xi_1, \xi_2, \xi_3), \qquad (\xi_1 < 0). \tag{7}$$

The initial condition is, at $t = 0$,

$$f = f_0, \tag{8}$$

where $f_0$ is properly chosen.

By use of properly chosen nondimensional variables, Eqs. (1)–(3c) and the boundary conditions (4a)–(7) are reduced to a system characterized by the four parameters: the Knudsen number $Kn[= (8RT_0/\pi)^{1/2}(A_c\rho_0)^{-1}D^{-1} = \ell_0/D]$, the Froude number $Fr(= 2RT_h/Dg)$, the temperature ratio $T_c/T_h$, and the aspect ratio $L/D$, where $\rho_0$ is the average density of the gas over the domain, $\ell_0$ is the mean free path of the state $f_e$ [in Eq. (2)] with $\rho = \rho_0$, $T = T_h$, and $v_i = 0$.

Equations (1)–(3c) with the boundary condition (4a)–(7) has a time-independent solution without flow $(v_i \equiv 0)$ for any set of the parameters. Let it be $f_s(X_2, \xi_i)$ and let the corresponding density and temperature be $\rho_s(X_2)$ and $T_s(X_2)$. When the gravity is strong (when $Fr$ is small), the density $\rho_s$ decreases as $X_2$ increases, but when the gravity is weak

(when $Fr$ is large), $\rho_s$ increases with $X_2$. In the intermediate gravity (intermediate $Fr$), $\rho_s$ first decreases with $X_2$, reaches its minimum, and then increases. Our interest is the possibility of another type of solutions with nonzero flow velocity, such as a steady solution of a convection roll, in a rarefied gas. Thus, we numerically analyze the initial and boundary-value problem (1)–(7) for many sets of parameters and investigate the range of parameters where solutions with flow exist, and their flow pattern. Further, we present an example of flow bifurcation, i.e., approach to different types of steady solutions from slightly different initial conditions.

The independent variable $\xi_3$ can be eliminated from the system (1)–(7), if we are satisfied with the information of the marginal distribution functions $\int_{-\infty}^{\infty} f d\xi_3$ and $\int_{-\infty}^{\infty} \xi_3^2 f d\xi_3$. The system for these quantities is obtained by integrating Eq. (1), (4a), (5a), (6), and (7) multiplied by 1 or $\xi_3^2$ with respect to $\xi_3$ over $(-\infty < \xi_3 < \infty)$. In the present work, we carry out a standard finite-difference numerical analysis of this system.

## III.    Existence range of nonstationary solutions and their flow patterns

In order to find the range of the parameters ($Fr$, $T_c/T_h$, etc.) where a flow occurs in the rectangular domain, we investigate the initial and boundary-value problem (1)–(7) for many sets of the parameters and pursue the long-time behavior of the solution. As the initial distribution function $f_0$ in Eq. (8), we take the Maxwellian distribution:

$$f_0 = \rho(2\pi RT)^{-3/2} \exp(-\xi_i^2/2RT),$$

$$\rho = \rho_s(X_2), \qquad T = T_s(X_2)[1 + (1/2)\cos(\pi X_1/L)\sin(\pi X_2/D)],$$

(9)

where $\rho_s(X_2)$ and $T_s(X_2)$ are the density and temperature of the stationary solution for the corresponding values of the parameters. (It is noted that the Maxwellian distribution with $\rho_s$ and $T_s$ is not the solution of Eq. (1) owing to its gravitational term.)

Pursuing the long-time behavior of the solution of the initial and boundary-value problem (1)–(7), we find that the solution approaches the corresponding stationary solution $f_s$ or a steady solution consisting of a single convection roll for all the cases computed. The

parameter range of the two class of solutions is shown in Figs. 1-3, where the stationary solution is marked by • and the steady solution of a convection roll by o in the $(Fr, T_c/T_h)$ plane. Fig. 1 is the result at $Kn = 0.02, 0.03, 0.04, 0.05$, and $0.06$ in the square domain $L/D = 1$, Fig. 2 is the result at $Kn = 0.02$ in the domain $L/D = 3/4$, and Fig. 3 is the result at $Kn = 0.02$ in the domain $L/D = 1/2$. A steady convection roll of flow exists in a triangular region in the $(Fr, T_c/T_h)$ plane, and it rapidly shrinks as the Knudsen number increases. According to the linear stability analysis[5] based on the continuum theory, $Ra \doteq 1700$, where $Ra = (16/\pi)(1 - T_c/T_h)/(T_c/T_h)Fr Kn^2$ (Rayleigh number), is the critical value above which the stationary solution is unstable. In Fig. 1 the curve $Ra = 1700$ is shown by a dashed line. As mentioned in Sec. II, the density $\rho_s(X_2)$ of a stationary solution decreases monotonically as $X_2$ increases for small $Fr$, but has its minimum in the gas for intermediate $Fr$. The approximate boundary of these regions is shown by a chain line in Fig. 1.

The computation is carried out only for a special initial condition. Thus, in the triangular region with o sign, a single roll of steady flow certainly exists, but another type of flow may occur. In fact we will show such examples, besides the reversal $f(L - X_1, X_2, -\xi_1, \xi_2, \xi_3)$ of a solution $f(X_1, X_2, \xi_1, \xi_2, \xi_3)$, in Sec. IV. In the region with • sign, the existence of a flow cannot be excluded, but various tests, although they are not systematic but are randomly carried out, show that occurrence of a perpetual flow is improbable.

Example of flow fields (flow velocity vectors, isodensity lines, and isothermal lines) in the case of $L/D = 1$ are shown in Figs. 4 and 5. In Fig. 4 the results at $Kn = 0.02$ and $T_c/T_h = 0.4$ are shown for three typical Froude numbers $Fr = 2, 3$, and $7.5$, which correspond to three different types of $\rho_s(X_2)$ mentioned in Sec. II. In Fig. 5 the results for two different Knudsen numbers, $Kn = 0.02$ and $0.04$ with the other parameters being common $(T_c/T_h = 0.1, Fr = 3)$ are shown. The lateral position of the center of the roll is nearly at $X_1 = 2L/3$ for all the cases in Figs. 4 and 5, but its vertical position differs appreciably depending on the parameters.

## IV.  Array of rolls and bifurcation of flow

A steady solution of Eq. (1) extended across a specularly reflecting plane boundary by joining its mirror image or reversal (i.e. extended symmetrically with respect to the boundary) can be shown to be a solution of Eq. (1) in a wider domain. Thus, by arranging a series of steady solutions of a kind laterally in such a way that adjacent solutions are the mirror images of each other, we can construct a steady solution in a wider domain. The array $f_a^N$ of $N$ steady solutions of a single roll $f_a$ in the domain with $L/D = a$ so arranged forms a solution consisting of $N$ rolls in the domain $L/D = Na$. For example both $f_{3/4}^4$ and $f_1^3$ are solutions in the domain $L/D = 3$.

Our next interest is bifurcation to these different types of flow. Taking, as the initial condition $f_0$ in the initial and boundary value problem (1)–(7) in the domain $L/D = k\ell/m$,

$$f_0 = \alpha f_{k/m}^\ell + (1 - \alpha)f_{\ell/m}^k ,\tag{10}$$

where $\alpha$ is a constant $(0 \leq \alpha \leq 1)$ and $k$, $\ell$, and $m$ are positive integers, we pursue the time-development of the solution and investigate the type of the limiting solution as $t \to \infty$ for different $\alpha$.

Here we give some results in the domain $L/D = 3$ for the initial condition (10) with $\ell = 4$, $k = 3$, and $m = 4$ for $Fr = 3$ and $T_c/T_h = 0.1$. When $Kn = 0.02$, the solution approaches $f_1^3$ for $\alpha = 0.6$ but $f_{3/4}^4$ for $\alpha = 0.7$; when $Kn = 0.03$, it approaches $f_1^3$ for $\alpha = 0.8$ but $f_{3/4}^4$ for $\alpha = 0.9$; when $Kn = 0.04$, even for $\alpha = 0.99$, it approaches $f_1^3$. Several tests indicate that if $f \to f_{3/4}^4$ for $\alpha_1$, then $f \to f_{3/4}^4$ for $\alpha \geq \alpha_1$ and that if $f \to f_1^3$ for $\alpha_2$, then $f \to f_1^3$ for $\alpha \leq \alpha_2$. The transition processes for $\alpha = 0.6$ and $0.7$ at $Kn = 0.02$ are shown in Fig. 6.

# References

1. Bénard, H. (1900): Les tourbillons cellulaires dans une nappe liquide. *Revue Gén. Sci. Pur. Appl.*, **11**, 1261-1271, 1309-1328.

2. Rayleigh, L. (1916): On convection currents in a horizontal layer of fluid when the higher temperature is on the under side. *Phil. Mag.*, **32**, 529-546.

3. Busse, F. H. and Clever, R. M. (1979): Instabilities of convection rolls in a fluid of moderate Prandtl number. *J. Fluid Mech.*, **91**, 319-335.

4. Mizushima, J. and Fujimura, K. (1992): Higher harmonic resonance of two-dimensional distributions in Rayleigh-Bénard convection. *J. Fluid Mech.*, **234**, 651-667.

5. Koschmieder, E. L. (1993): *Bénard Cells and Taylor Vortices*. Cambridge Univ. Press, Cambridge.

6. Cercignani, C. and Stefanov, S. (1992): Bénard's instability in kinetic theory. *Transp. Theory Stat. Phys.*, **21**, 371-381; Stefanov, S. and Cercignani, C. (1992): Monte Carlo simulation of Bénard's instability in a rarefied gas. *Eur. J. Mech., B/Fluids*, **11**, 543-554.

7. Bird, G. A. (1976): *Molecular Gas Dynamics*. Clarendon Press, Oxford.

8. Sone, Y. and Aoki, K. (1994): *Molecular Gas Dynamics* (Appendix II). Asakura, Tokyo.

9. Bhatnagar, P. L., Gross, E. P. and Krook, M. (1954): A model for collision processes in gases, I. *Phys. Rev.*, **94**, 511-525.

10. Welander, P. (1954): On the temperature jump in a rarefied gas. *Ark. Fys.* **7**, 507-553.
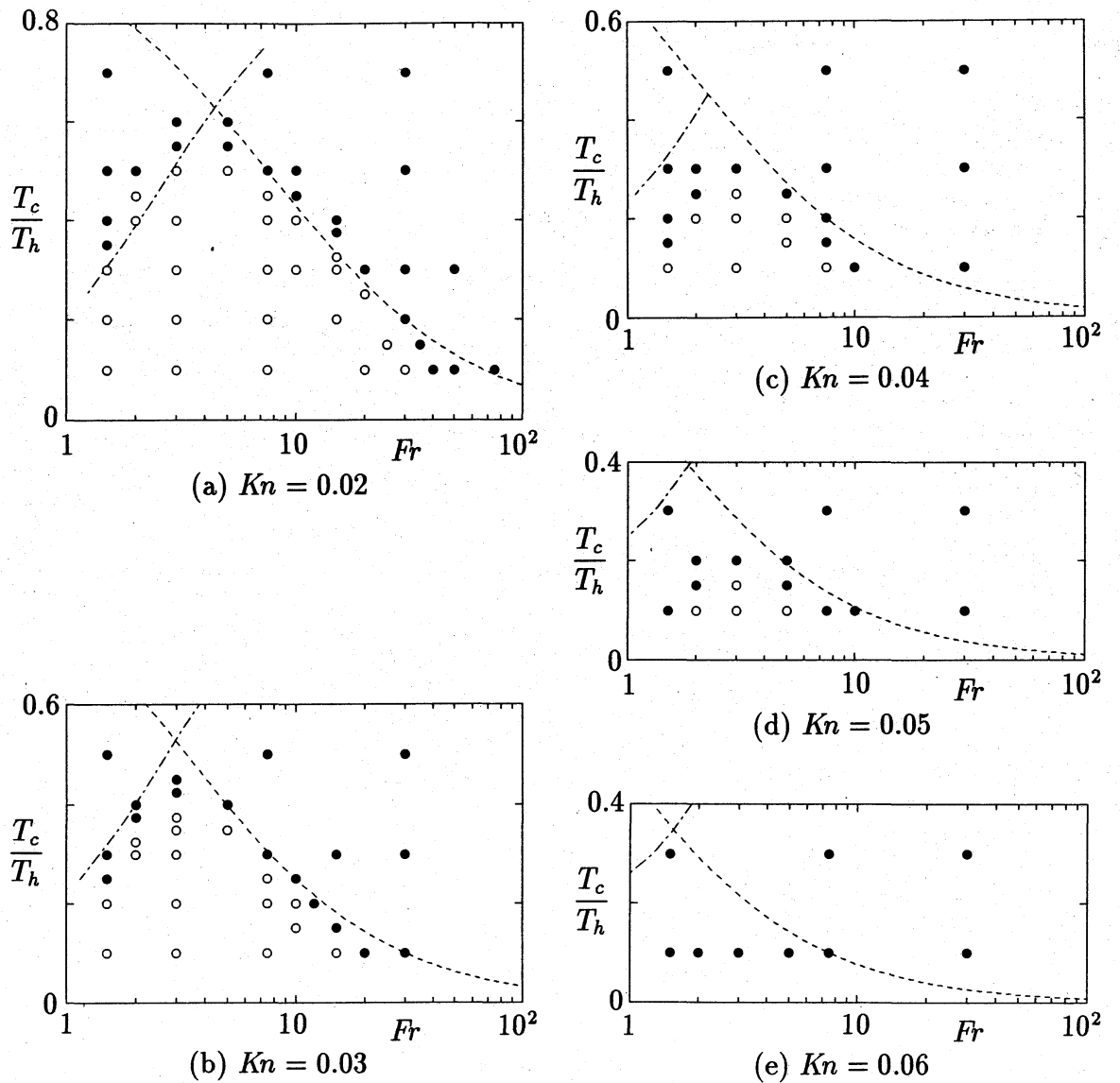
152



Fig. 1. The range of the parameters $Fr$ and $T_c/T_h$ where a convection roll exists for $L/D = 1$. (a) $Kn = 0.02$, (b) $Kn = 0.03$, (c) $Kn = 0.04$, (d) $Kn = 0.05$, and (e) $Kn = 0.06$. o : Convection occurs; ● : No flow occurs. See the second paragraph in Sec. III for ---- and ------ . [The $(X_1, X_2)$ space is divided into 24×24 nonuniform rectangular lattices finer near the upper and right boundaries. The $(\xi_1, \xi_2)$ space, limited to $|\xi_1|$ and $|\xi_2| \leq 4(2RT_h)^{1/2}$, is divided into 40×40 nonuniform rectangular lattices, finer near the lines $\xi_1 = 0$ and $\xi_2 = 0$.]

153



Fig. 2. The range of the parameters $Fr$ and $T_c/T_h$ where a convection roll exists for $L/D = 3/4$ and $Kn = 0.02$. o : Convection occurs; • : No flow occurs. (See the caption of Fig. 1 for the lattice system.)
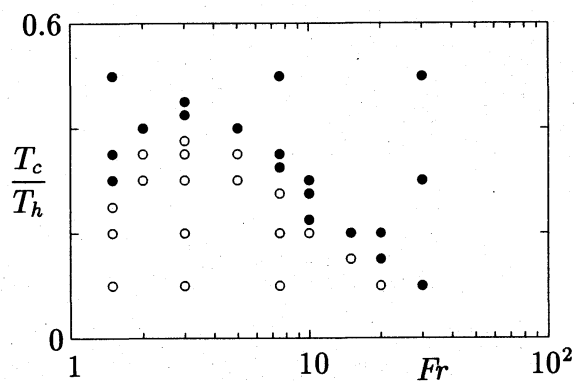


Fig. 3. The range of the parameters $Fr$ and $T_c/T_h$ where a convection roll exists for $L/D = 1/2$ and $Kn = 0.02$. o : Convection occurs; • : No flow occurs. (See the caption of Fig. 1 for the lattice system.)
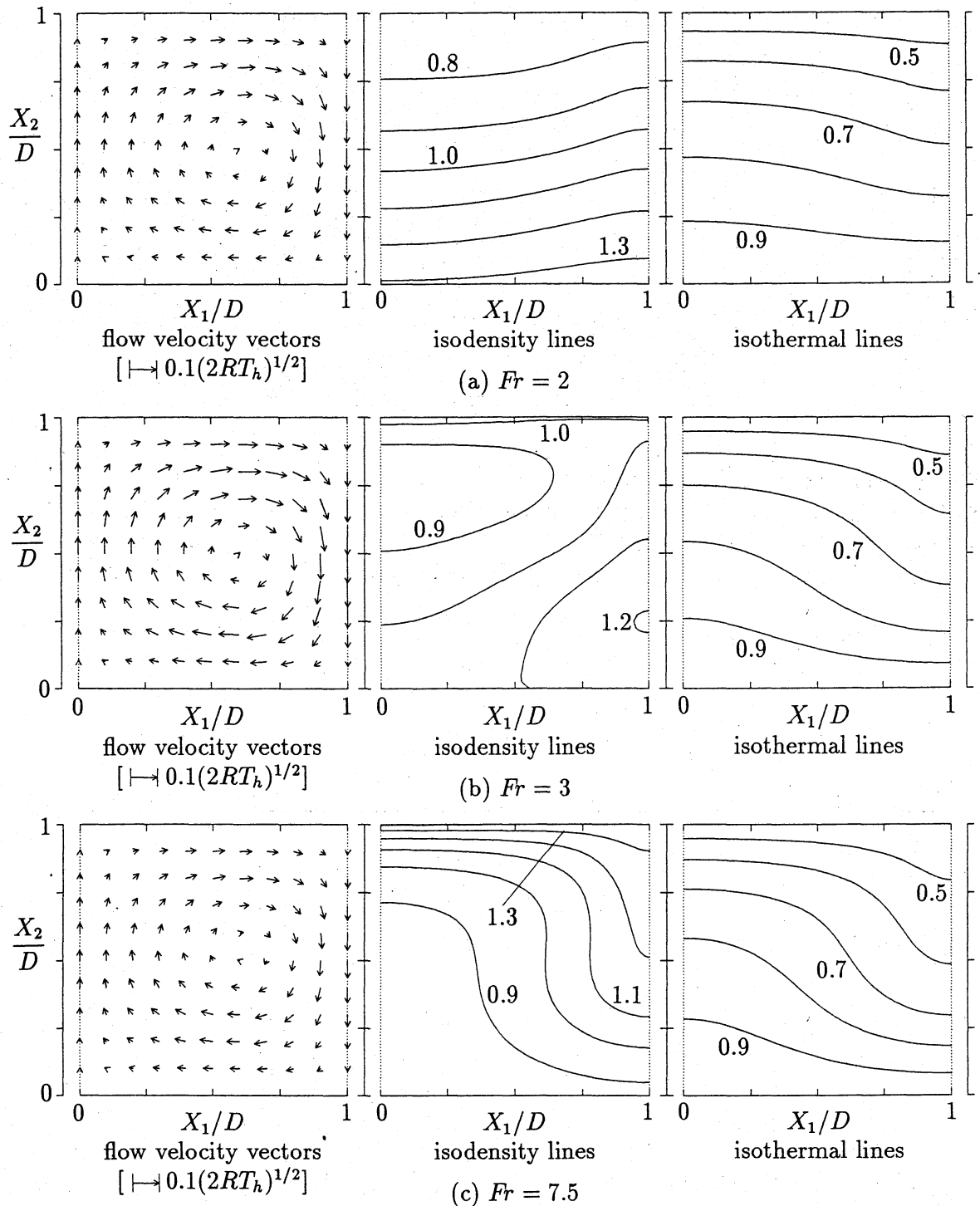
Fig. 4. Flow velocity vectors, isodensity lines, and isothermal lines for three Froude numbers, $Fr$ = 2, 3, and 7.5, with $L/D$ = 1, $Kn$ = 0.02, and $T_c/T_h$ = 0.4. (a) $Fr$ = 2, (b) $Fr$ = 3, and (c) $Fr$ = 7.5. The arrows indicate the velocity at their starting points. The contours $\rho/\rho_0 = 0.1n$ and $T/T_h = 0.1n$ are shown. [The $(X_1, X_2)$ space is divided into 48×48 [in (a) and (b)] or 72×72 [in (c)] nonuniform rectangular lattices finer near the upper and right boundaries. The $(\xi_1, \xi_2)$ space, limited to $|\xi_1|$ and $|\xi_2| \leq 4(2RT_h)^{1/2}$, is divided into 40×80 [in (a)], 40×60 [in (b)], or 40×40 [in (c)] nonuniform rectangular lattices, finer near the lines $\xi_1$ = 0 and $\xi_2$ = 0. ]
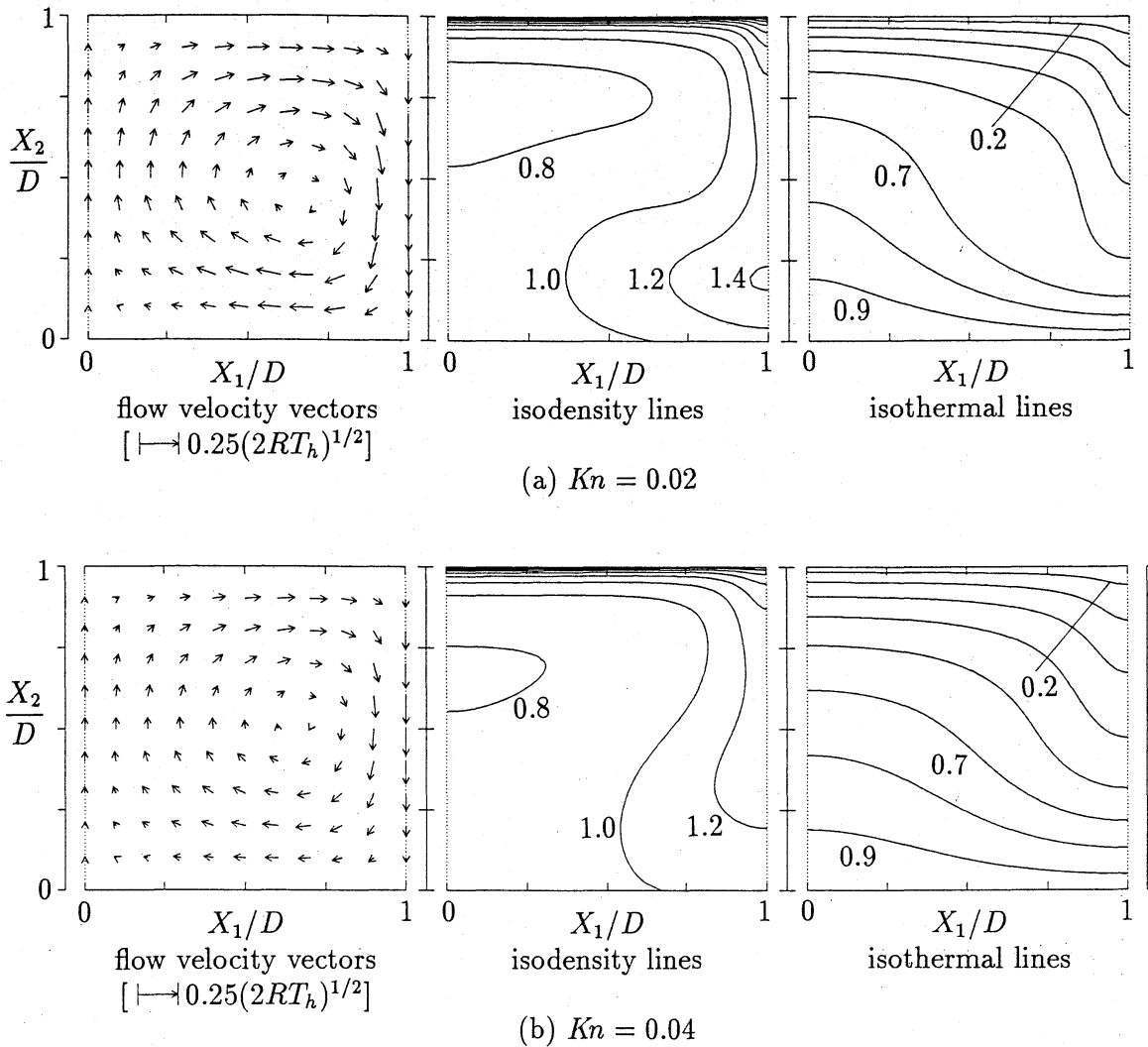
Fig. 5. Flow velocity vectors, isodensity lines, and isothermal lines for two Knudsen numbers, $Kn = 0.02$ and $0.04$, with $L/D = 1$, $Fr = 3$, and $T_c/T_h = 0.1$. (a) $Kn = 0.02$ and (b) $Kn = 0.04$. The arrows indicate the velocity at their starting points. The contours $\rho/\rho_0 = 0.2n$ and $T/T_h = 0.1n$ are shown. [The $(X_1, X_2)$ space is divided into $48 \times 56$ nonuniform rectangular lattices finer near the upper and right boundaries. The $(\xi_1, \xi_2)$ space, limited to $|\xi_1|$ and $|\xi_2| \leq 4(2RT_h)^{1/2}$, is divided into $40 \times 60$ nonuniform rectangular lattices, finer near the lines $\xi_1 = 0$ and $\xi_2 = 0$. ]
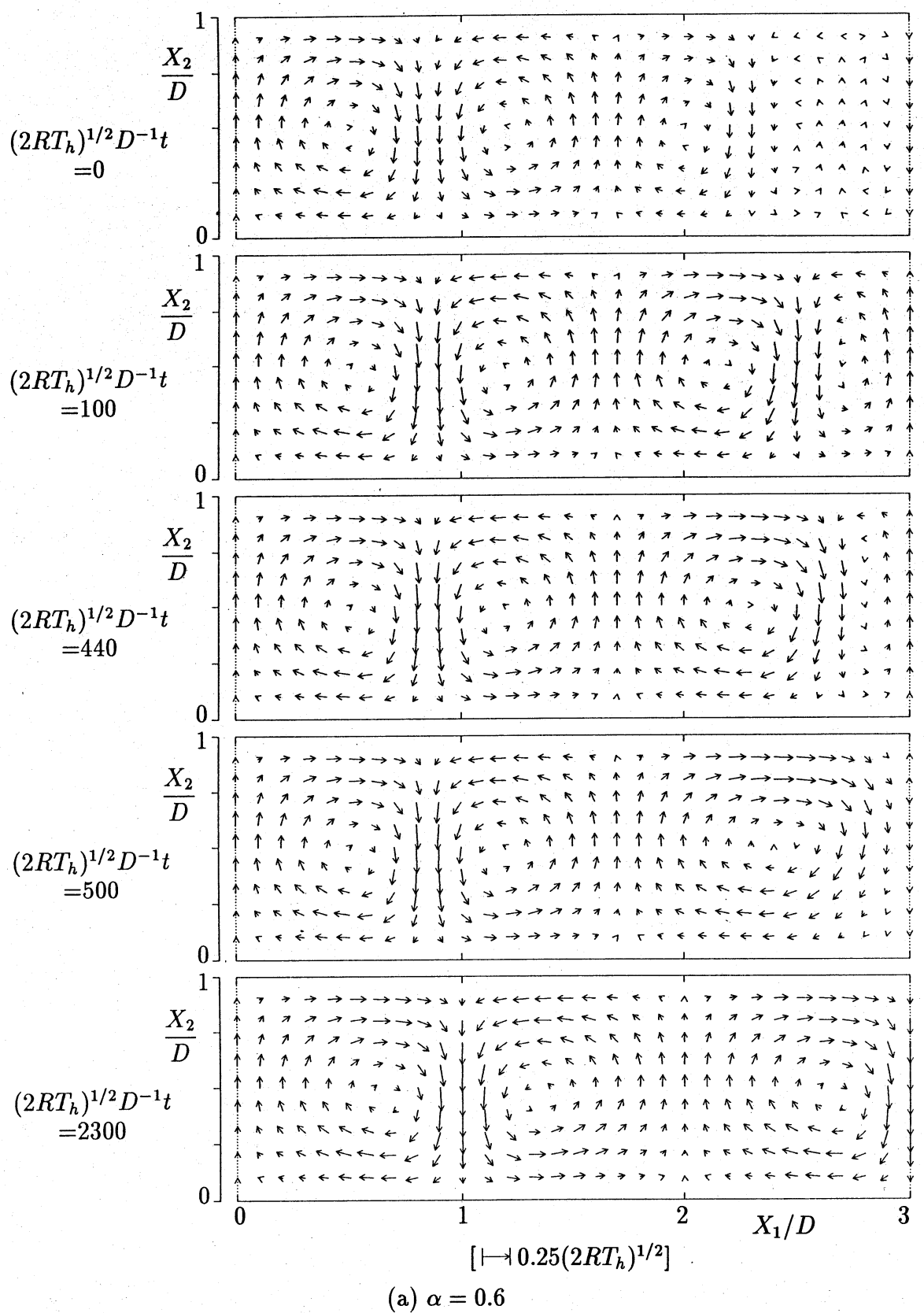
$[\,\vdash\!\!\!\rightarrow 0.25(2RT_h)^{1/2}]$

(a) $\alpha = 0.6$

Fig. 6. (See the next page for the caption.)

$[\vdash\dashv 0.25(2RT_h)^{1/2}]$
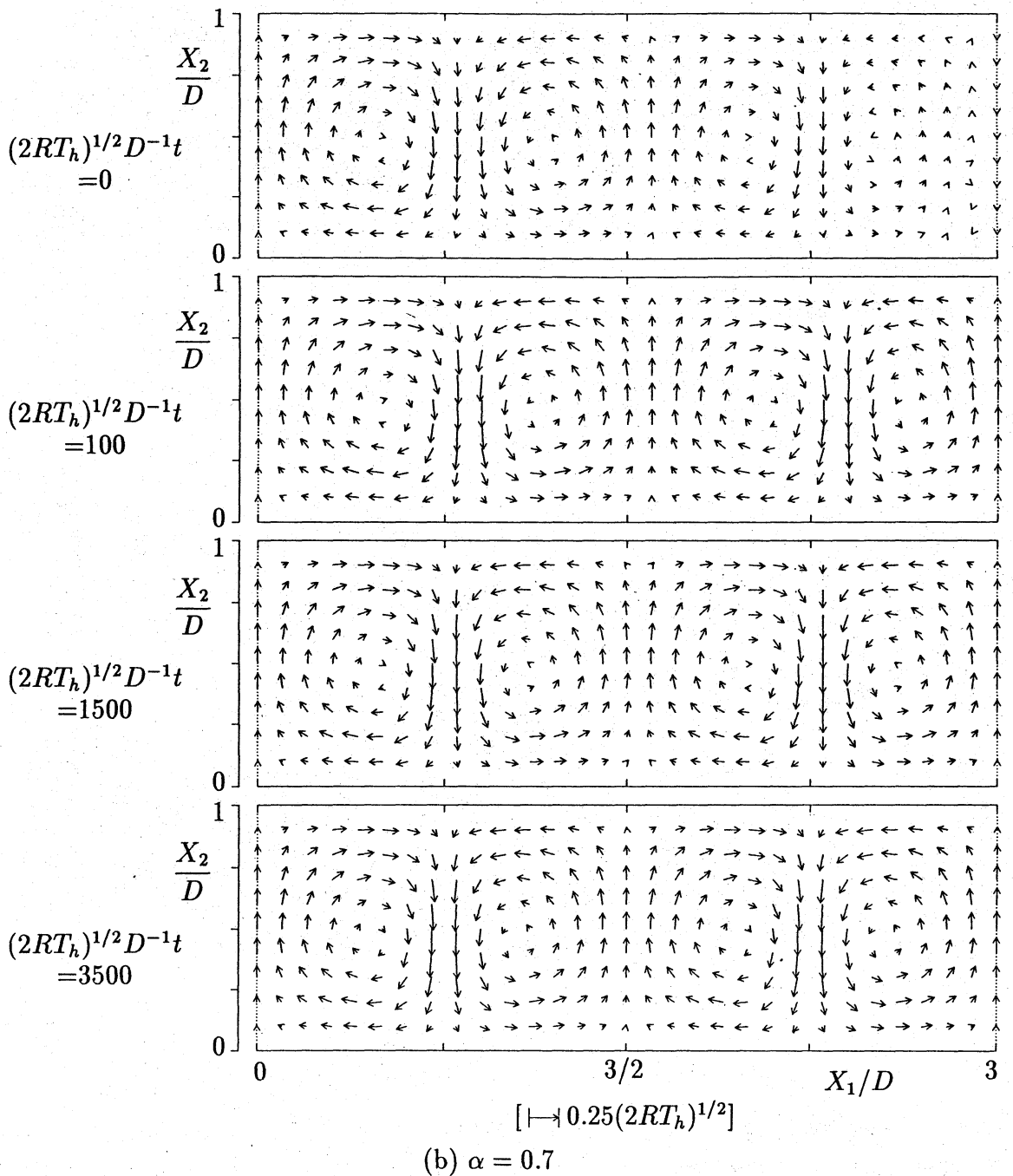
(b) $\alpha = 0.7$

Fig. 6. Bifurcation of flow for $L/D = 3$, $Kn = 0.02$, $Fr = 3$, and $T_c/T_h = 0.1$. (a) $\alpha = 0.6$ and (b) $\alpha = 0.7$. The time-development of velocity fields of the initial and boundary-value problem (1)-(8) with (10) is shown. The arrows indicate the velocity at their starting points. In (b) the most right "roll" is smallest at about $t(2RT_h)^{1/2}/D = 50 \sim 100$. [The $(X_1, X_2)$ space is divided into 96×28 rectangular lattices uniform in $X_1$ and nonuniform in $X_2$ (finer near the upper boundary). The $(\xi_1, \xi_2)$ space, limited to $|\xi_1|$ and $|\xi_2| \leq 4(2RT_h)^{1/2}$, is divided into 40×40 nonuniform rectangular lattices, finer near the lines $\xi_1 = 0$ and $\xi_2 = 0$. The time step $\Delta t$ is $\Delta t = 0.1D/(2RT_h)^{1/2}$. For accurate description of the initial stage, more detailed computation with a finer time step is required. ]